Revised ESI for manuscript (CE-ART-11-2018-001925.R1)

Electronic Supplementary Information (ESI)

Two 2D microporous MOFs based on bent carboxylates and linear spacer for selective CO_2 adsorption

Arun Pal[†], Antarip Mitra[†], Santanu Chand[†], Jian-Bin Lin[‡] and Madhab C. Das[†]*

[†]*Department of Chemistry, Indian Institute of Technology Kharagpur, 721302, W.B., India.*
[‡]*Department of Chemistry, University of Calgary, Calgary, Alberta T2N 1N4, Canada.*
E-mail: mcdas@chem.iitkgp.ac.in

Physical Measurements. FTIR spectra were measured on a Perkin-Elmer RX1 spectrophotometer in the wavenumber range of 4000 to 400 cm^{-1}. Elemental analyses (C, H, N and S) were carried out on an Elementar, Vario Micro Cube elemental analyzer. Powder XRD data were collected with *Cu-*K_α radiation on a Bruker D8 Advance diffactometer in the range of 2θ = 5-50°. Thermogravimetric analysis (TGA) experiments were studied on a TG 209 *F3* Tarsus (Netzsch) from room temperature to 800 ℃ at 5 ℃/min under N_2 atmosphere. ^1H, ^{13}C-NMR spectrum was recorded on a Bruker Avance II 400 spectrometer. Mass (MALDI-TOF) spectrum was recorded using a Bruker MALDI-TOF/TOF mass spectrometer. Gas sorption experiments were tested on a Micromeritics 3-Flex Surface Characterization Analyzer at different temperatures. To remove all the guest solvents in the framework, the fresh samples were first solvent-exchanged with dry chloroform at least 10 times within two days and degassed at 343 K for 12 h until the outgas rate was 5 μmHg/min prior to measurements. The sorption measurement was maintained at 77 K under liquid nitrogen and at 195 K by using methanol/dry ice mixture. A chiller was used for adsorption isotherms at 273 and 295 K, respectively.

Single Crystal X-ray Diffraction. The single-crystal X-ray diffraction data were collected with Mo-K_α radiation (λ = 0.71073 Å) on a Bruker SMART APEX II CCD diffractomete at 298 K for **1** and **2**. The absorption correction was carried out using the SADABS program. The structures were solved by direct methods, and the non-hydrogen atoms were refined anisotropically by the SHELXTL software package with full-matrix least-squares procedure.[1] The highly disordered guest solvent molecules for **2** in void volume can be removed by PLATON/SQUEEZE.[2] The crystal, refinement data, selected bond lengths and angles of complexes **1-2** are summarized in Table S1 and S2, ESI, respectively.

Table S1: Crystal data and structure refinements for MOFs **1-2**.

	1	**2**
Empirical formula	$C_{29}H_{25}CdN_5O_7$	$C_{40}H_{26}N_4O_{13}S_2Zn_2$
Formula weight	667.94	965.51
Temperature (K)	298 (1)	298 (1)
Radiation	Mo-Kα	Mo-Kα
Wavelength (λ)	0.71073Å	0.71073Å
Crystal system	Triclinic	Triclinic
Space group	$P\bar{1}$	$P1$
a [Å]	9.949 (5)	9.894 (5)
b [Å]	11.344 (5)	12.719 (5)
c [Å]	12.395 (5)	12.789 (5)
α [°]	98.565 (5)	60.037 (5)
β [°]	90.042 (5)	77.603 (5)
γ [°]	91.149 (5)	83.457 (5)
Volume [Å^3]	1383.0 (11)	1361.7 (10)
Z	2	1
Density (calculated) [Mg/m^3]	1.604	1.177
Absorption coefficient [mm^{-1}]	0.847	1.011
F (000)	676	490
Refl. used [$I > 2\sigma(I)$]	3921	4218
Independent reflections	6908	6001
R_{int}	0.0730	0.0542
Refinement method	full-matrix least squares on F^2	full-matrix least squares on F^2
GOF	0.961	1.019
Final R indices [I>2σ(I)]	R_1= 0.0527; wR_2= 0.0977	R_1= 0.0617; wR_2= 0.1734
R indices (all data)	R_1= 0.1283; wR_2= 0.1266	R_1= 0.0889; wR_2= 0.1893
CCDC No	1877080	1877081

Table S2: Selected Bond Distances (Å) and Bond Angles (°) in **1** **2**.

		1			
Cd1	O1	2.327(4)	Cd1 O2	2.337(3)	Cd1 N4	2.339(4)
Cd1	N1	2.357(4)	Cd1 O3	2.369(3)	Cd1 O4	2.397(3)
Cd1	O1	2.585(3)				

O1	Cd1 O2	124.28(12)	O2	Cd1 O4	88.25(12)
O1	Cd1 N4	91.67(14)	N4	Cd1 O4	86.79(13)
O2	Cd1 N4	99.77(13)	N1	Cd1 O4	96.85(13)
O1	Cd1 N1	83.31(13)	O3	Cd1 O4	54.74(11)
O2	Cd1 N1	83.99(12)	O1	Cd1 O1	74.46(12)

N4 Cd1 N1	174.87(15)	O2 Cd1 O1	52.58(11)
O1 Cd1 O3	92.55(12)	N4 Cd1 O1	85.98(12)
O2 Cd1 O3	140.40(13)	N1 Cd1 O1	93.65(12)
N4 Cd1 O3	92.36(13)	O3 Cd1 O1	166.83(11)
N1 Cd1 O3	86.84(13)	O4 Cd1 O1	138.01(11)
O1 Cd1 O4	147.10(11)		

		2			
Zn1 O3	2.011(10)	Zn1 O7	2.064(9)	Zn1 O5	2.068(8)
Zn1 O1	2.085(10)	Zn1 N4	2.125(10)	Zn2 N1	1.910(13)
Zn2 O4	2.006(11)	Zn2 O6	2.044(10)	Zn2 O8	2.063(9)
Zn2 O2	2.083(11)				

O3 Zn1 O7	87.8(4)	N1 Zn2 O4	101.2(5)
O3 Zn1 O5	161.0(4)	N1 Zn2 O6	102.9(5)
O7 Zn1 O5	87.0(4)	O4 Zn2 O6	155.6(4)
O3 Zn1 O1	91.8(4)	N1 Zn2 O8	99.7(5)
O7 Zn1 O1	158.5(4)	O4 Zn2 O8	87.1(4)
O5 Zn1 O1	86.4(4)	O6 Zn2 O8	85.2(4)
O3 Zn1 N4	101.1(4)	N1 Zn2 O2	101.1(5)
O7 Zn1 N4	93.1(4)	O4 Zn2 O2	91.0(5)
O5 Zn1 N4	97.4(4)	O6 Zn2 O2	88.1(4)
O1 Zn1 N4	108.1(4)	O8 Zn2 O2	159.1(4)

Table S3: Non-bonding interactions in **1-2**.

Complex-**1**			
D-H...A	d(H…A) (Å)	D(D…A) (Å)	∠ DHA (^{O})
C6 H6…O7	2.615	3.361	137.54
C12 H12…O6	2.702	3.342	126.68
C16 H16…O7	2.553	3.201	127.16
C23 H23…O4	2.577	3.417	150.42
N3 H3N3…O4	2.125	2.919	167.12

Complex-**2**			
D-H...A	d(H…A) (Å)	D(D…A) (Å)	∠ DHA (^{O})
C2 H2…O1	2.605	3.404	144.41
C3 H3…O11	2.553	3.411	153.34
C5 H5…O12	2.571	3.045	112.06
C9 H9…O5	2.510	3.154	126.52
C11 H11…O8	2.330	3.244	167.53
C21 H21…O13	2.424	3.276	152.31

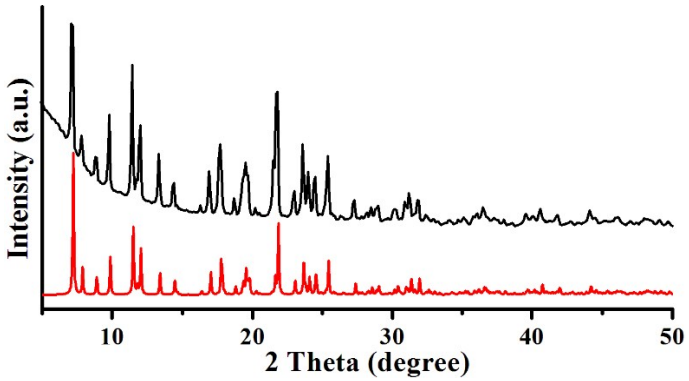

Figure S1: Simulated (red) and as synthesized (black) PXRD pattern of **1**.

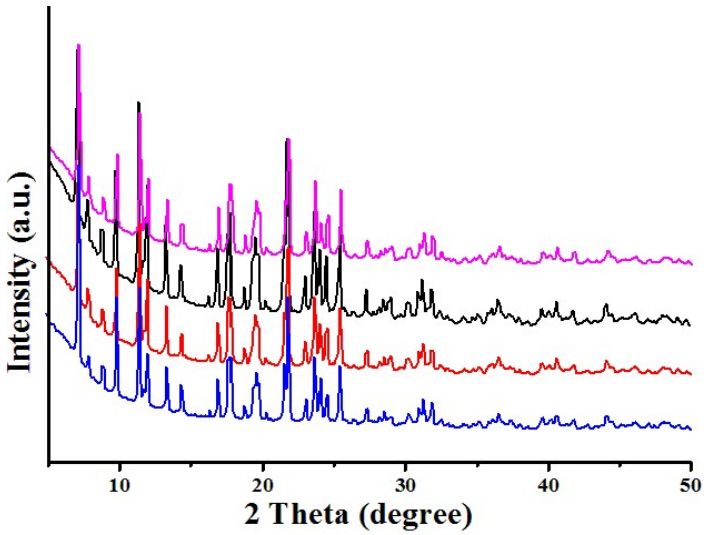

Figure S2: As synthesized (blue), chloroform exchanged (red), desolvated (black) and after CO_2 adsorption (magenta) PXRD pattern of **1**.

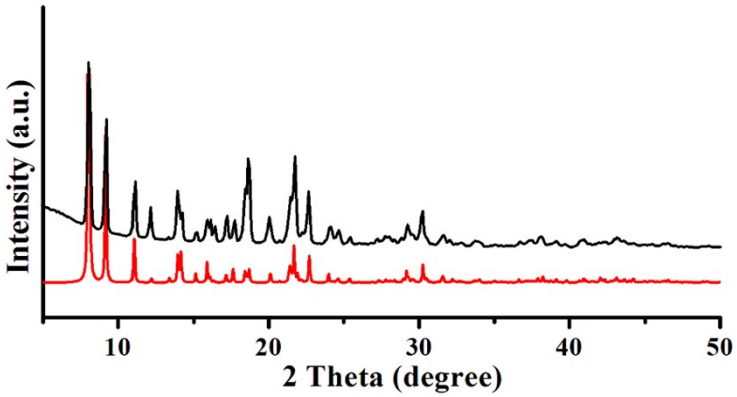

Figure S3: Simulated (red) and as synthesized (black) PXRD pattern of **2**.

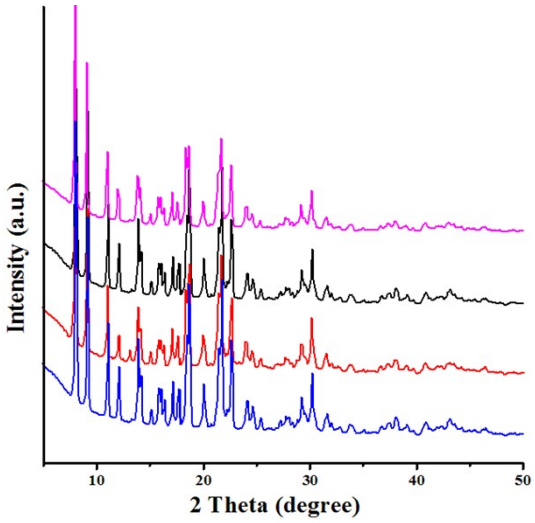

Figure S4: As synthesized (blue), chloroform exchanged (red), desolvated (black) and after CO_2 adsorption (magenta) PXRD pattern of **2**.

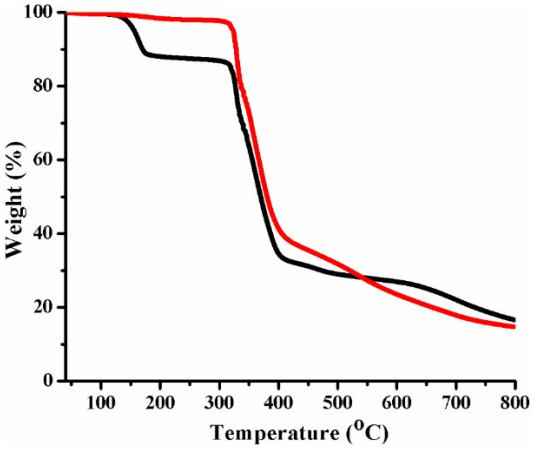

Figure S5: TGA of as-synthesized (black) and after gas adsorption (red) **1**.

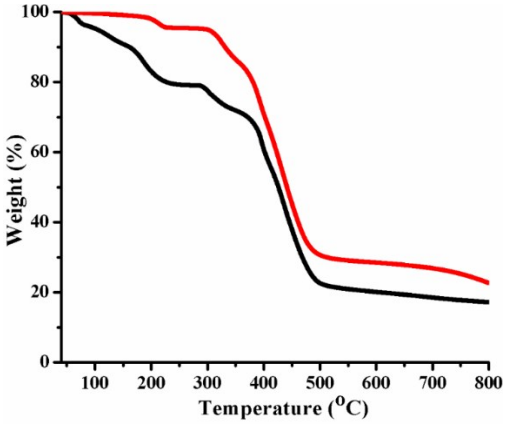

Figure S6: TGA of as-synthesized (black) and after gas adsorption (red) **2**.

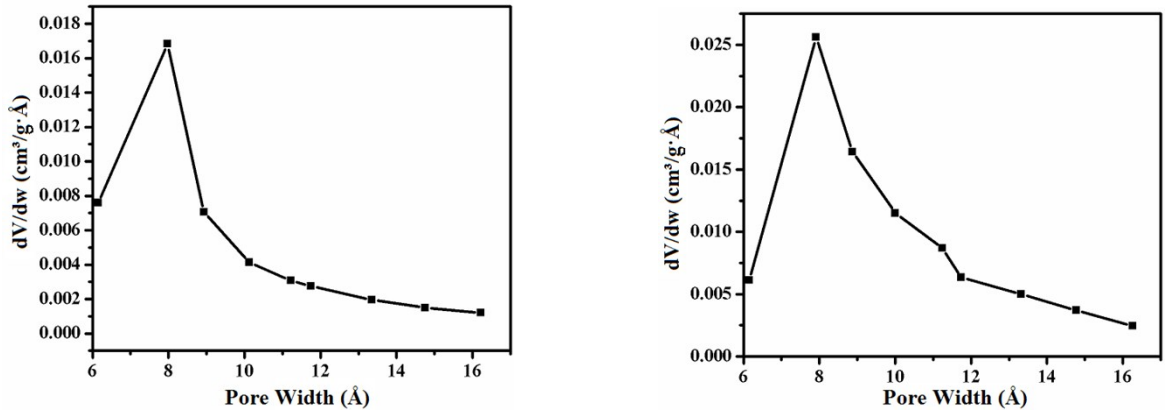

Figure S7: The pore size distributions for **1** (a) and **2** (b) derived from the 195 K CO_2 isotherms by applying Horvath-Kawazoe analysis.

Calculation of Isosteric Heats of Adsorption:

The isosteric heats of adsorption (Q_{st}) were calculated using the Clausius-Clapeyron equation based on pure-component isotherms collected at two different temperatures of 273 K and 295 K. The Q_{st} was defined as

$$Q_{st} = -R\left(\frac{\partial lnx}{\partial\left(\frac{1}{T}\right)}\right)_y$$

Where x is the pressure, T is the temperature, R is the gas constant and y is the adsorption amount. These calculations are done through the "Heat of Adsorption" function embedded in the software supplied by Micromeritics 3- Flex Surface Characterization Analyzer.

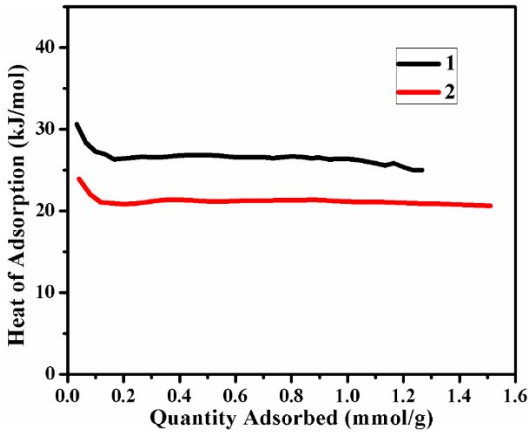

Figure S8: Isosteric heat of CO_2 (Q_{st}) of **1** and **2**.

Table S4: Q_{st} data for CO_2 adsorption of some selected MOFs.

MOFs	Q_{st} (kJ/mol)	Reference
1	**30.6**	**This work**
2	**24**	**This work**
[Cu(Me-4pytrz-ia)]	30	3(a)
PCN-88	27	3(b)
Cu-TPBTM	26	3(c)
$[Co_2Cl_2(bbta)]$	28	3(d)
ZTF-1	25.4	3(e)
SIFSIX-1-Cu	27	3(f)
SIFSIX-2-Cu	21	3(f)
$[Cu(bcppm)H_2O]$	29	3(g)
IITKGP-5	22.6	3(h)
IITKGP-6	23	3(i)
HHU-3	24.6	3(j)
HHU-5	25.6	3(j)
NOTT-125	25.35	3(j)
ZJNU-54	24.7	3(j)
ZJU-8	21.9	3(j)
UTSA-5	28.1	3(k)
UTSA-49	27	3(l)
IPM-MOF-110	32	3(m)
JUC-141	27.85	3(n)
ZIF-78	29	3(o)

Calculation of CO_2/N_2 and CO_2/CH_4 Selectivity (IAST Selectivity):

Adsorption isotherms and gas selectivities of mixed CO_2/N_2 (15:85) and CO_2/CH_4 (50:50) at different temperatures were calculated based on the ideal adsorbed solution theory (IAST) proposed by Myers and Prausnitz.[4] In order to calculate the selective sorption performance of **1** and **2** toward the separation of binary mixed gases, the parameters fitted from the single-component CO_2, CH_4 and N_2 adsorption isotherms based on the dual-site Langmuir−Freundlich (DSLF) model and were used in the IAST calculations as given below in detail.[5]

$$y = \frac{q_{m1} b_1 x^{1/n_1}}{1 + b_1 x^{1/n_1}} + \frac{q_{m2} b_2 x^{1/n_2}}{1 + b_2 x^{1/n_2}}$$

Where x is the pressure of the bulk gas at equilibrium with the adsorbed phase (kPa); y is the adsorbed amount per mass of adsorbent (mmol/g), q_{m1} and q_{m2} are the saturation capacities of sites 1 and 2 (mmol/g); b_1 and b_2 are the affinity coefficients of sites 1 and 2 (1/kPa), n_1 and n_2 represent the deviations from an ideal homogeneous surface. The fitting parameters of DSLF equation are listed in Table S5-S6.

The predicted adsorption selectivity is defined as

$$S = \left(\frac{x_1}{y_1} \middle/ \frac{x_2}{y_2} \right)$$

Where x_i and y_i are the mole fractions of component i (i = 1, 2) in the adsorbed and bulk phases, respectively. The IAST calculations were carried out for a binary mixture containing 15% CO_2 (y_1) and 85% N_2 (y_2), which is typical of flue gases and for a binary mixture containing 50% CO_2 (y_1) and 50% CH_4 (y_2), which is typical of landfill gases.

Table S5: Equation parameters for the DSLF isotherm model of **1**.

Adsorbates	q_{m1} (mmol/g)	b_1 (1/kPa)	n_1	q_{m2}(mmol/g)	b_2 (1/kPa)	n_2
CO_2 (273K)	0.3652	0.00448	0.97898	1.49765	0.0618	0.91894
CH_4 (273K)	1.62863	0.0012	0.7229	0.11899	0.05085	0.7739
N_2(273K)	1.17985	0.00102	0.88918	0.01391	1.66033E-30	0.0686

CO_2(295K)	0.51	1.55704E-18	0.98	1.69899	0.02374	0.9672
CH_4(295K)	0.15882	0.03144	0.90095	1.27772	2.96783E-4	0.6075
N_2(295K)	0.26296	1.47856E-4	0.59325	0.02079	0.00188	0.53862

Table S6: Equation parameters for the DSLF isotherm model of **2**.

Adsorbates	q_{m1} (mmol/g)	b_1 (1/kPa)	n_1	q_{m2} (mmol/g)	b_2 (1/kPa)	n_2
CO_2 (273K)	1.96724	0.00709	0.97489	1.16623	0.06025	0.92714
CH_4 (273K)	1.64608	0.00682	0.89879	0.19425	0.0579	0.88992
N_2(273K)	1.18208	0.00261	0.94672	0.00472	2.60513E-30	0.06198
CO_2(295K)	1.87897	0.00519	0.9454	0.90519	0.03627	0.94899
CH_4(295K)	3.00578	4.77937E-4	0.97268	1.44787	0.00773	0.98839
N_2(295K)	0.7102	6.71552E-4	0.7296	0.04865	0.02482	0.88512

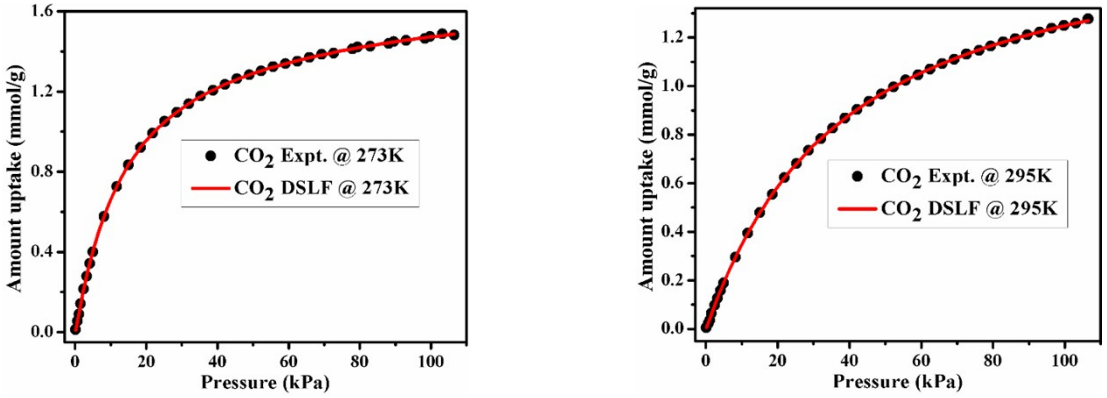

(a) **(b)**

Figure S9: Duel-site Langmuir-Freundlich fitting (red line) for CO_2 (black circle) isotherms measured at 273 K (a) and 295 K (b) of **1**.

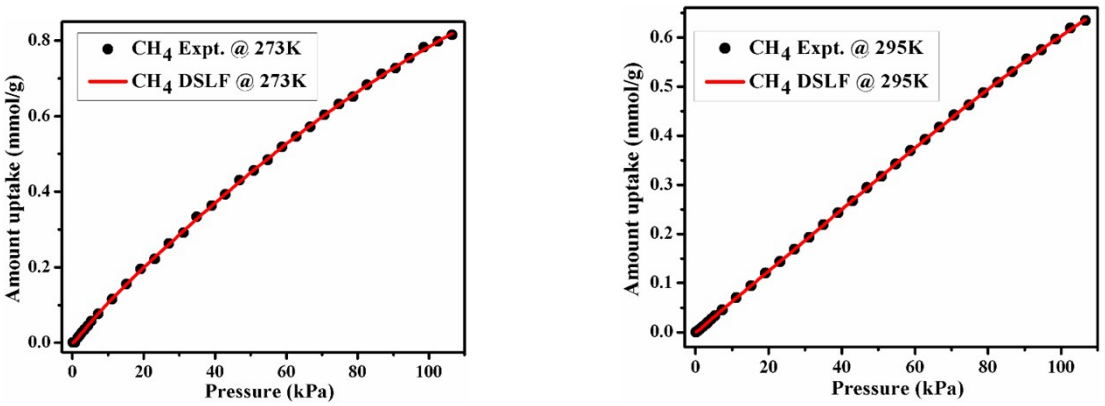

(a) **(b)**

Figure S10: Duel-site Langmuir-Freundlich fitting (red line) for CH_4 (black circle) isotherms measured at 273 K (a) and 295 K (b) of **1**.

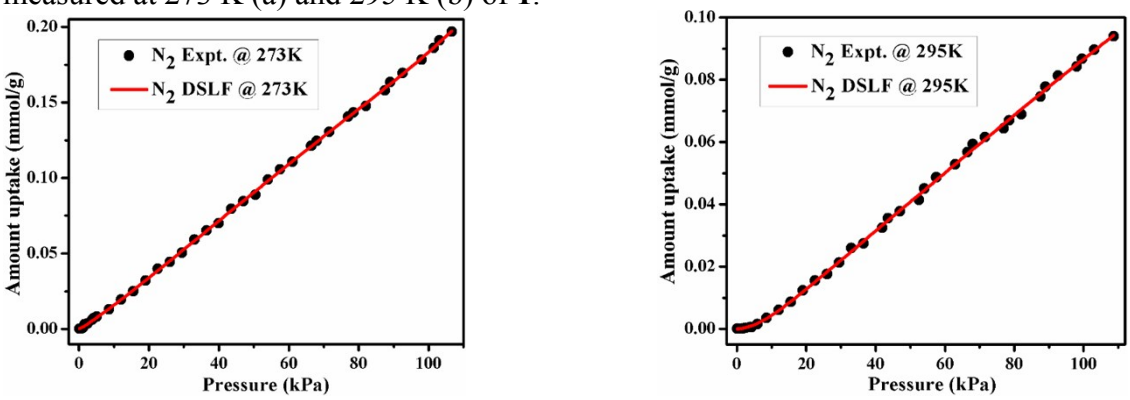

(a) **(b)**

Figure S11: Duel-site Langmuir-Freundlich fitting (red line) for N_2 (black circle) isotherms measured at 273 K (a) and 295 K (b) of **1**.

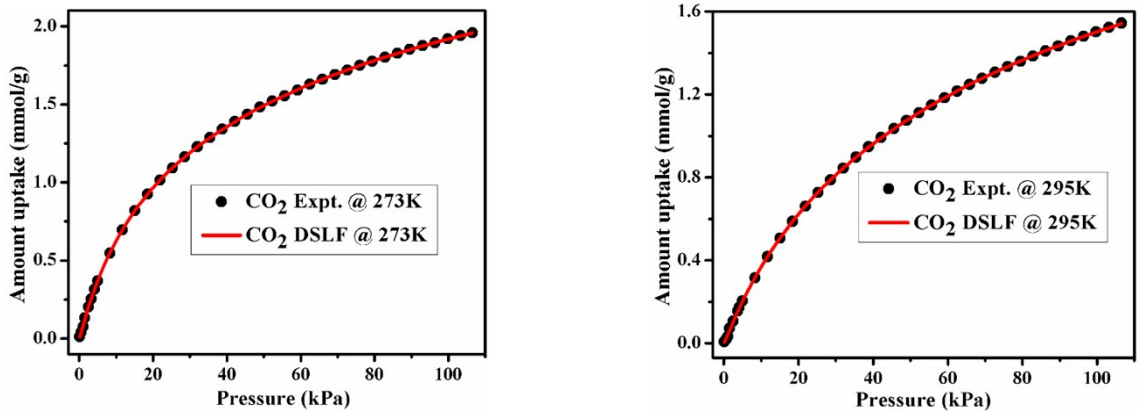

(a) **(b)**

Figure S12: Duel-site Langmuir-Freundlich fittings (red line) for CO_2 (black circle) isotherms measured at 273 K (a) and 295 K (b) of **2**.

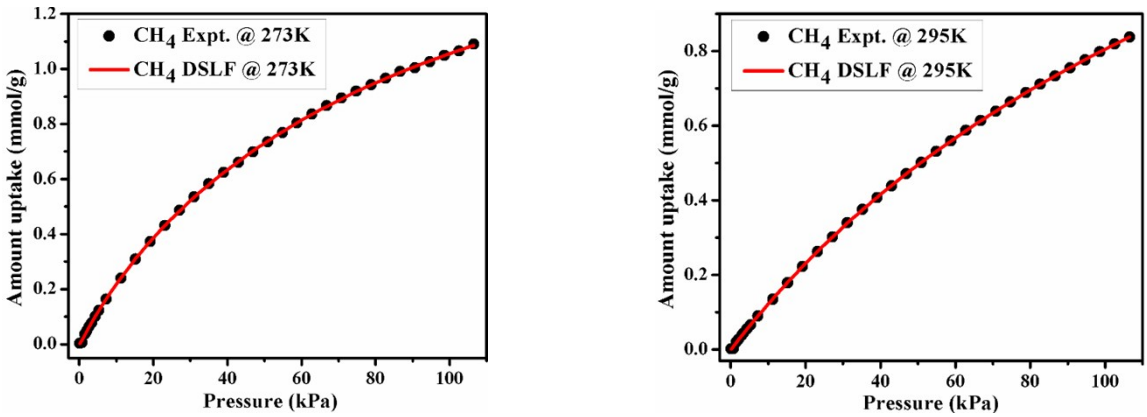

(a) **(b)**

Figure S13: Duel-site Langmuir-Freundlich fitting (red line) for CH_4 (black circle) isotherms measured at 273 K (a) and 295 K (b) of **2**.

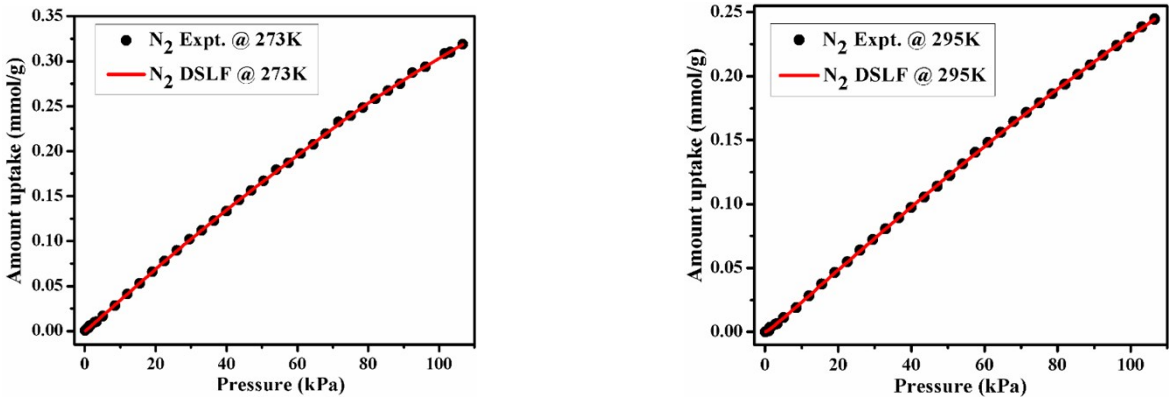

(a) **(b)**

Figure S14: Duel-site Langmuir-Freundlich fitting (red line) for N_2 (black circle) isotherms measured at 273 K (a) and 295 K (b) of **2**.

Table S7: Adsorption selectivity of reported MOFs for CO_2/N_2 (15:85) and CO_2/CH_4 (50:50) at 1 bar (a: IAST selectivity; b: selectivity from Henry's Law; c: From slopes of adsorption isotherms at low pressure).

Compound	CO_2/N_2 adsorption selectivity	CO_2/CH_4 adsorption selectivity	Temperature (K)	Reference
1	**51**[a]	**7.3**[a]	**273**	**This work**
	75.7[a]	**5**[a]	**295**	**This work**
2	**27.6**[a]	**4.1**[a]	**273**	**This work**
	18.4[a]	**3.4**[a]	**295**	**This work**

SIFSIX-2-Cu	13.7[a]	5.3[a]	298	6(a)
SIFSIX-1-Cu	27[a]	11[a]	298	6(a)
TIFSIX-1-Cu	30[a]	11[a]	298	6(b)
SNFSIX-1-Cu	22[a]	12[a]	298	6(b)
PCN-88	18[a]	5[a]	296	6(c)
PCN-61	15[a]		298	3(c)
$Cu_{24}(TPBTM)_8$	22[a]		298	3(c)
ZJNU-44a	15[a]	5.5[a]	296	6(d)
UTSA-72a	48.3[a]		273	6(e)
	35.6[a]		296	
UTSA-85a	55[a]		273	6(f)
	62.5[a]		296	
PMOF-3a	29.2[a]	8[a]	273	6(g)
	23.4[a]	5.1[a]	296	
JUC-141	21.62[a]	4.20[a]	273	3(n)
	27.60[a]	8.72[a]	298	
Zn-MOF-74		5[a]	296	6(h)
MOF-177	3.6[a]		296	6(h)
Cu-BTTri	21[a]		298	6(i)
en-Cu-BTTri	25[a]		298	6(i)
NOTT-202a	26.7[b]	2.9[b]	273	6(j)
	4.3[b]	1.4[b]	293	
ZIF-68	18.7[c]	5[c]	298	3(o)
ZIF-69	19.9[c]	5.1[c]	298	3(o)
ZIF-70	17.3[c]	5.2[c]	298	3(o)
ZIF-79	23.2[c]	5.4[c]	298	3(o)
ZIF-81	23.8[c]	5.7[c]	298	3(o)
ZIF-95	18±1.7[c]	4.3±0.4[c]	298	3(o)

References:

1. Bruker, SMART and SAINT (Bruker AXS Inc, Madison, Wisconsin, 2007).

2. Platon Program: A. L. Spek, *Acta Crystallogr., Sect. A* 1990, **46**, 194.

3. (a) D. Lässig, J. Lincke, J. Moellmer, C. Reichenbach, A. Moeller, R. Gläser, G. Kalies, K. A. Cychosz, M. Thommes, R. Staudt and H. Krautscheid, *Angew. Chem., Int. Ed.,* 2011, **50**, 10344–10348; (b) J.-R. Li, J. Yu, W. Lu, L.-B. Sun, J. Sculley, P. B. Balbuena and H.-C. Zhou, *Nat. Commun.,* 2012, **4**, 1538; (c) B. Zheng, J. Bai, J. Duan, L. Wojtas and M. J. Zaworotko, *J. Am. Chem. Soc*., 2011, **133**, 748-751; (d) P.-Q. Liao, H. Chen, D.-D. Zhou, S.-Y. Liu, C.-T. He, Z. Rui, H. Ji, J.-P. Zhang and X.-M. Chen, *Energy Environ. Sci.,* 2015, **8**, 1011–1016; (e) T, Panda, P. Pachfule, Y. Chen, J. Jiang and R. Banerjee, *Chem. Commun*., 2011, **47**, 2011-2013; (f) S. D. Burd, S. Ma, J. A. Perman, B. J. Sikora, R. Q. Snurr, P. K. Thallapally, J. Tian, L. Wojtas, M. J. Zaworotko, *J. Am. Chem. Soc.* 2012, **134**, 3663–3666; (g) W. M. Bloch, R. Babarao, M. R. Hill, C. J. Doonan and C. J. Sumby, *J. Am. Chem. Soc.,* 2013, **135**, 10441–10448; (h) A. Pal, S. Chand, S. M. Elahi and M. C. Das, *Dalton Trans.,* 2017, **46**, 15280-15286; (i) A. Pal, S. Chand and M. C. Das, *Inorg. Chem.,* 2017, **56**, 13991-13997; (j) Z. Lu, F. Meng, L. Du, W. Jiang, H. Cao, J. Duan, H. Huang and H. He, *Inorg. Chem*., 2018, DOI: 10.1021/acs.inorgchem.8b02031; (k) G. Chen, Z. Zhang, S. Xiang and B. Chen, *CrystEngComm*, 2013, **15**, 5232–5235; (l) S. Xiong, Y. Gong, H. Wang, H. Wang, Q. Liu, M. Gu, X. Wang, B. Chen and Z. Wang, *Chem. Commun*. 2014, **50**, 12101-12104; (m) S. Mukherjee, R. Babarao, A. V. Desai, B. Manna and S. K. Ghosh, *Cryst. Growth Des.,* 2017, **17**, 3581-3587; (n) N. Zhao, F. Sun, P. Li, X. Mu and G. Zhu, *Inorg. Chem*., 2017, **56**, 6938-6942; (o) A. Phan, C. J. Doonan, F. J. Uribe-Romo, C. B. Knobler, M. O'Keeffe and O. M. Yaghi, *Acc. Chem. Res*., 2010, **43**, 58-67.

4. A. L. Myers and J. M. Prausnitz, *AIChE J.,* 1965, **11**, 121.

5. B. Li, Y. Zhang, R. Krishna, K. Yao, Y. Han, Z. Wu, D. Ma, Z. Shi, T. Pham, B. Space, J. Liu, P. K.Thallapally, J. Liu, M. Chrzanowski and S. Ma, *J. Am. Chem. Soc*., 2014, **136**, 8654.

6. (a) P. Nugent, Y. Belmabkhout, S. D. Burd, A. J. Cairns, R. Luebke, K. Forrest, T. Pham, S. Ma, B. Space, L. Wojtas, M. Eddaoudi and M. J. Zaworotko, *Nature*, 2013, **495**, 80-84; (b) P. Nugent, V. Rhodus, T. Pham, B. Tudor, K. Forrest, L. Wojtas, B. Space and M. Zaworotko, *Chem. Commun*., 2013, **49**, 1606-1608; (c) J. -R. Li, J. Yu, W. Lu, L.-B. Sun, J. Sculley, P. B. Balbuena and H.-C. Zhou, *Nat. Commun*., 2013, **4**, 204-212; (d) C. Song, J. Hu, Y. Ling, Y. L. Feng, R. Krishna, D. Chen and Y. He, *J. Mater. Chem. A*, 2015, **3**, 19417-19426; (e) H. Alawisi,

B. Li, Y. He, H. D. Arman, A. M. Asiri, H. Wang and B. Chen, *Cryst. Growth Des*., 2014, **14**, 2522-2526; (f) O. Alduhaish, H. Wang, B. Li, H. D. Arman, V. Nesterov, K. Alfooty and B. Chen, *ChemPlusChem*, 2016, **81**, 764-769; (g) O. Alduhaish, H. Wang, B. Li, T. –L. Hu, H. D. Arman, K. Alfooty and B. Chen, *ChemPlusChem*, 2016, **81**, 770-774; (h) S. Xiang, Y. He, Z. Zhang, H. Wu, W. Zhou, R. Krishna and B. Chen, *Nat. Commun*., 2012, **3**, 954-963; (i) A. Demessence, D. M. D'Alessandro, M. L. Foo and J. R. Long, *J. Am. Chem. Soc*., 2009, **131**, 8784-8786; (j) S. Yang, X. Lin, W. Lewis, M. Suyetin, E. Bichoutskaia, J. E. Parker, C. C. Tang, D. R. Allan, P. J. Rizkallah, P. Hubberstey, N. R. Champness, K. M. Thomas, A. J. Blake and M. Schröder, *Nat. Mater*, 2012, **11**, 710-716.